*Inorg. Chem.* **2004**, *43*, 7353–7358

# Multi-Iron Silicotungstates: Synthesis, Characterization, and Stability Studies of Polyoxometalate Dimers

**Travis M. Anderson, Wade A. Neiwert,† Kenneth I. Hardcastle, and Craig L. Hill***

*Department of Chemistry, Emory University, Atlanta, Georgia 30322*

Received April 13, 2004

The reaction of Fe(III) with $Na^+$ and $K^+$ salts of the trivacant $[\alpha\text{-}SiW_9O_{34}]^{10-}$ ligand have been investigated at pH 6 and pH 1. A new dimer, $[(\alpha\text{-}SiFe_3W_9(OH)_3O_{34})_2(OH)_3]^{11-}$ (**1**), is synthesized by reacting $Na_7H_3[\alpha\text{-}SiW_9O_{34}]$ or $K_{10}[\alpha\text{-}SiW_9O_{34}]$ with exactly 3 equiv of Fe(III) in a 0.5 M sodium acetate solution (pH 6). The structure of **1**, determined by single-crystal X-ray diffraction ($a = 22.454(2)$ Å, $b = 12.387(2)$ Å, $c = 37.421(2)$, $\beta = 100.107(8)°$, monoclinic, $C2/c$, $Z = 4$, $R_1 = 5.11\%$ based on 12739 independent reflections), consists of two $[\alpha\text{-}SiFe_3W_9(OH)_3O_{34}]^{4-}$ units linked by three Fe–$\mu$-OH–Fe bonds. Reaction of $K_{10}[\alpha\text{-}SiW_9O_{34}]$ with 3 equiv of Fe(III) in water (pH 1) yields $[(\alpha\text{-}Si(FeOH_2)_2FeW_9(OH)_3O_{34})_2]^{8-}$ (**2**). The structure of **2** was also determined by single-crystal X-ray diffraction ($a = 36.903(2)$ Å, $b = 13.9868(9)$ Å, $c = 21.7839(13)$ Å, $\beta = 122.709(1)°$, monoclinic, $C2/c$, $Z = 4$, $R_1 = 4.57\%$ based on 11787 independent reflections). It consists of two $[\alpha\text{-}Si(FeOH_2)_2FeW_9(OH)_3O_{34}]^{4-}$ Keggin units linked by a single edge. The terminal ligand on Fe1 in each trisubstituted Keggin unit becomes a $\mu_2$ oxo ligand bridging to a $[WO_6]^{2-}$ moiety. The UV–vis spectra of both complexes show the characteristic oxygen-to-metal-charge-transfer bands of polyoxometalates as well as an Fe(III)-centered band at 436 nm ($\epsilon = 146$ $M^{-1}$ $cm^{-1}$) and 456 nm ($\epsilon = 104$ $M^{-1}$ $cm^{-1}$) for complexes **1** and **2**, respectively. Differential scanning calorimetry data show that complex **1** decomposes between 575 and 600 °C whereas no decomposition is observed for complex **2** up to temperatures of 600 °C.

## Introduction

The chemistry of d-electron-transition-metal-substituted polyoxometalates (POMs), sometimes referred to as inorganic metalloporphyrins, continues to attract much interest, particularly with respect to redox- and acid-dependent catalysis, but also with respect to medicinal and materials applications as well.[1,2] The development of POMs as catalysts derives in part from the fact that they consist of a close-packed array of oxide anions, and, as such, can function as tractable homogeneous representations of metal oxides and metal oxide heterogeneous oxidation catalysts.[3] Much research has focused on trivacant lacunary Keggin moieties because they define the largest possible planar minisurface on the plenary $XW_{12}O_{40}^{n-}$ (X = tetrahedral heteroatom) polyanion.[4]

Reactions of the A-type trivacant Keggin POMs, $SiW_9O_{34}^{10-}$ (Figure S1A) and $PW_9O_{34}^{9-}$ (Figure S1B), with d-electron-transition-metal cations are complex, and a number of different structures have been reported.[5−13] Initially, Pope

* To whom correspondence should be addressed. E-mail: chill@emory.edu.
† Current address: Department of Chemistry, Bethel University, St. Paul, Minnesota 55112.

(1) Pope, M. T. *Heteropoly and Isopoly Oxometalates*; Springer-Verlag: Berlin, 1983.
(2) Recent reviews of POMs include: (a) Contant, R.; Hervé, G. *Rev. Inorg. Chem.* **2002**, *22*, 63−111. (b) Pope, M. T. Polyoxo Anions: Synthesis and Structure. In *Comprehensive Coordination Chemistry II: Transition Metal Groups 3−6*; Wedd, A. G., Ed.; Elsevier Science: New York, 2004; Vol. 4, Chapter 4.10, pp 635−678. (c) Hill, C. L. Polyoxometalates: Reactivity. In *Comprehensive Coordination Chemistry II: Transition Metal Groups 3−6*; Wedd, A. G., Ed.; Elsevier Science: New York, 2004; Vol. 4, Chapter 4.11, pp 679−759.
(3) Representative work includes: (a) Finke, R. G.; Droege, M. W. *J. Am. Chem. Soc.* **1984**, *106*, 7274−7277. (b) Day, V. W.; Klemperer, W. G. *Science* **1985**, *228*, 533−541. (c) Lyon, D. K.; Finke, R. G. *Inorg. Chem.* **1990**, *29*, 1789−1791. (d) Anderson, T. M.; Hill, C. L. *Inorg. Chem.* **2002**, *41*, 4252−4258.
(4) Representative papers include: (a) Finke, R. G.; Droege, M.; Hutchinson, J. R.; Gansow, O. *J. Am. Chem. Soc.* **1981**, *103*, 1587−1589. (b) Finke, R. G.; Droege, M. W.; Domaille, P. J. *Inorg. Chem.* **1987**, *26*, 3886−3896. (c) Clemente-Juan, J. M.; Coronado, E.; Galán-Mascarós, J. R.; Gómez-García, C. J. *Inorg. Chem.* **1999**, *38*, 55−63. (d) Kortz, U.; Isber, S.; Dickman, M. H.; Ravot, D. *Inorg. Chem.* **2000**, *39*, 2915−2922. (e) Ritorto, M. D.; Anderson, T. M.; Neiwert, W. A.; Hill, C. L. *Inorg. Chem.* **2004**, *43*, 44−49.
(5) The A-type trivacant Keggin structure is formed by removing one corner-sharing $WO_6$ octahedron from each of three bridging $M_3O_{13}$ triads while the B-type isomer is formed by removing one entire $M_3O_{13}$ triad from the plenary $XW_{12}O_{40}^{n-}$ structure.
(6) Katsoulis, D. E.; Pope, M. T. *J. Am. Chem. Soc.* **1984**, *106*, 2737−2738.
(7) Liu, J.; Ortéga, F.; Sethuraman, P.; Katsoulis, D. E.; Costello, C. E.; Pope, M. T. *J. Chem. Soc., Dalton Trans.* **1992**, 1901−1906.

10.1021/ic049517s CCC: $27.50 
Published on Web 10/12/2004

and co-workers reported that $Na_7H_3[\alpha\text{-}SiW_9O_{34}]$ (and $Na_9H[\beta\text{-}SiW_9O_{34}]$) reacts with d-metal cations (M) to yield a mixture of $[\alpha\text{-}SiM_3W_9O_{37}]^{n-}$ (and $[\beta\text{-}SiM_3W_9O_{37}]^{n-}$) and the dimeric species, $[(\alpha\text{-}SiM_3W_9O_{37})_2(OH)_3]^{(2n+3)-}$ (and $[(\beta\text{-}SiM_3W_9O_{37})_2(OH)_3]^{(2n+3)-}$).[6,7] Subsequently, Knoth reported that the phosphorus analogue, $Na_8H[\beta\text{-}PW_9O_{34}]$, reacts with divalent d-metal cations (in the presence of $K^+$) to form sandwich-type complexes, $[M_3(\alpha\text{-}PW_9O_{34})_2]^{12-}$.[8,9]

Recently, Hervé and co-workers reported the synthesis and crystal structure of the $K^+$ salt of $\alpha\text{-}SiW_9O_{34}^{10-}$.[10] In this salt, two $\alpha\text{-}SiW_9O_{34}^{10-}$ moieties are linked via a set of six $K^+$ cations to form a dimer.[11] In contrast, the crystal structure of the $Na^+$ salt of $\alpha\text{-}SiW_9O_{34}^{10-}$ reveals that the $\alpha\text{-}SiW_9O_{34}^{10-}$ units do not associate to form a dimer, and the terminal oxygen atoms of the vacant W(VI) sites are protonated and consequently cannot interact with the $Na^+$ countercations.[12] Likewise, acidification of $K_{10}[\alpha\text{-}SiW_9O_{34}]$ in aqueous solution yields a new open Wells−Dawson structure, $\alpha\text{-}Si_2W_{18}O_{66}^{16-}$ (Figure S1C) whereas acidification of $Na_7H_3[\alpha\text{-}SiW_9O_{34}]$ gives only the monolacunary species, $\alpha\text{-}SiW_{11}O_{39}^{8-}$.[13,14]

As part of a program initially aimed at preparing multi-iron POMs as catalysts for ambient temperature, $O_2$/air-based oxidation of sulfides, aldehydes, and alkenes, we have investigated the synthesis and characterization of two new complexes, $K_4Na_7[(\alpha\text{-}SiFe_3W_9(OH)_3O_{34})_2(OH)_3]$ (**1**) and $K_2Na_6[(\alpha\text{-}Si(FeOH_2)_2FeW_9(OH)_3O_{34})_2]$ (**2**) (Figure 1).[15] These compounds are characterized by single-crystal X-ray structural analysis as well as infrared and electronic spectroscopy, differential scanning calorimetry, room-temperature magnetic susceptibility, and elemental (and thermogravimetric) analyses. The results show that differences in the acid sensitivities of the two trivacant precursors, $Na_7H_3[\alpha\text{-}SiW_9O_{34}]$ and $K_{10}[\alpha\text{-}SiW_9O_{34}]$, may be exploited to obtain high yields of trisubstituted dimeric and monomeric complexes, respectively.

## Experimental Section

**General Methods and Materials.** $K_{10}[\alpha\text{-}SiW_9O_{34}]\cdot 24H_2O$ and $Na_{10}[\alpha\text{-}SiW_9O_{34}]\cdot 18H_2O$ were obtained by published procedures, and purity was confirmed by infrared spectroscopy and elemental analysis.[10,16] Elemental analyses of Fe, K, Na, Si, and W were performed by Kanti Labs (Mississauga, Canada) and Desert Analytics (Tucson, Arizona). Infrared spectra (2% sample in KBr) were recorded on a Nicolet 510 instrument. The electronic absorption spectra were taken on a Hewlett-Packard 8452A UV−vis spectrophotometer. Average magnetic susceptibilities were measured on a Johnson-Matthey model MSB-1 magnetic susceptibility balance as neat powders at 24 °C; the balance was calibrated using $Hg[Co(SCN)_4]$ as a standard. Pascal's constants were used to obtain the final diamagnetic corrections. Differential scanning calorimetric and thermogravimetric data were collected on ISI DSC 550 and TGA 1000 instruments, respectively.

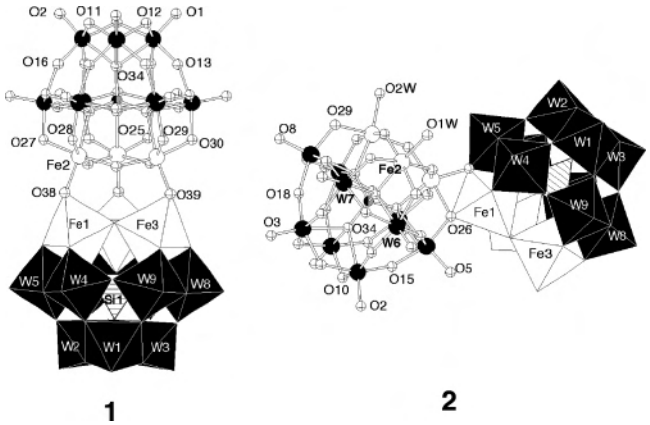


**Figure 1.** Ball-and-stick/polyhedral representations of $[(\alpha\text{-}SiFe_3W_9(OH)_3O_{34})_2(OH)_3]^{11-}$ (**1**) and $[(\alpha\text{-}Si(FeOH_2)_2FeW_9(OH)_3O_{34})_2]^{8-}$ (**2**).

**Synthesis of $K_4Na_7[(\alpha\text{-}SiFe_3W_9(OH)_3O_{34})_2(OH)_3]\cdot 36H_2O$ (1).** A 8.7 g (21.6 mmol) sample of $Fe(NO_3)_3\cdot 9H_2O$ was dissolved in 300 mL of 0.5 M sodium acetate in an 800 mL beaker, and the solution was heated to 70 °C. A 20 g (7.19 mmol) sample of $Na_{10}[SiW_9O_{34}]\cdot 18H_2O$ was slowly added to the Fe(III) solution with vigorous stirring. The final pH of the solution is ∼6. Any insoluble material that is present is removed by filtration with Celite, and a solution of 6.5 g of KCl dissolved in 25 mL of $H_2O$ is added to the resulting filtrate. A yellow-brown solid is removed by filtration and recrystallized to obtain the bulk pure sample (yield 70%). Green, diffraction quality crystals formed in the resulting filtrate after approximately 7 days (yield ∼10%). IR (2% KBr pellet, 1200−400 $cm^{-1}$): 1150 (w), 994 (w), 951 (m), 901 (s), 876 (s, sh), 797 (w), 768 (w), 704 (w), and 521 (m). Electronic spectral data (400−700 nm, in $H_2O$ (4 mM sample, 1 cm cell path length)) [$\lambda$, nm ($\epsilon$, $M^{-1}$ $cm^{-1}$)]: 436 nm (146). Magnetic susceptibility: $\mu_{eff} = 8.1$ $\mu_B$/mol at 295 K. Anal. Calcd for $K_4Na_7[(\alpha\text{-}SiFe_3W_9(OH)_3O_{34})_2(OH)_3]\cdot 27H_2O$ (for a sample dried in vacuo for 12 h): Fe, 5.84; K, 2.73; Na, 2.81; ($OH_2$), 8.5; Si, 0.98; W, 57.69. Found: Fe, 5.91; K, 2.76; Na, 2.79; ($OH_2$), 8.4; Si, 0.95; W, 56.71. [MW = 5736 g/mol].

**Synthesis of $K_2Na_6[(\alpha\text{-}Si(FeOH_2)_2FeW_9(OH)_3O_{34})_2]\cdot 27H_2O$ (2).** A 0.84 g (2 mmol) sample of $Fe(NO_3)_3\cdot 9H_2O$ was dissolved in 25 mL of $H_2O$ at room temperature in a 150 mL beaker. A 2 g (0.67 mmol) sample of $K_{10}[SiW_9O_{34}]\cdot 24H_2O$ was suspended in 15 mL of $H_2O$ and quickly added to the Fe(III) solution with vigorous stirring. The final pH of the solution is 1. Any insoluble material that is present is removed by filtration, 1 mL of 4 M NaCl is added to the resulting filtrate, and the clear, yellow solution is left to crystallize at room temperature. Diffraction quality crystals formed after approximately 7 days (yield ∼40%). IR (2% KBr pellet,

(8) Knoth, W. H.; Domaille, P. J.; Farlee, R. D. *Organometallics* **1985**, *4*, 62−68.
(9) Knoth, W. H.; Domaille, P. J.; Harlow, R. L. *Inorg. Chem.* **1986**, *25*, 1577−1584.
(10) Laronze, N.; Marrot, J.; Hervé, G. *Inorg. Chem.* **2003**, *42*, 5857−5862.
(11) In the crystal structure of $K_{10}[(\alpha\text{-}SiW_9O_{34})]\cdot 24H_2O$, two $\alpha\text{-}SiW_9O_{34}^{10-}$ moieties are linked in an eclipsed fashion. In contrast, the crystal structure of the $\beta$-isomer ($Na^+$ salt) reveals that the two $\beta\text{-}SiW_9O_{34}^{10-}$ units are linked in a staggered fashion (Figure S1A). See ref 10 and the following: Robert, F.; Tézé, A. *Acta Crystallogr.* **1981**, *B37*, 318−322.
(12) Hubert, V.; Hartl, H. *Z. Naturforsch.* **1996**, *B51*, 969−974.
(13) Laronze, N.; Marrot, J.; Hervé, G. *J. Chem. Soc., Chem. Commun.* **2003**, 2360−2361.
(14) An X-ray structure of the phosphorus analogue ($Na_{12}H_4[\beta\text{-}PW_9O_{34}\text{-}Na(H_2O)]_2\cdot 38H_2O$) is also known (Figure S1B). See: He, J.; Chen, Y.; Wang, X.; Fang, X.; Liu, J. *J. Mol. Struct.* **2002**, *641*, 159−164.
(15) Recent work on multi-iron POMs as catalysts for $O_2$/air-based oxidations includes: (a) Nishiyama, Y.; Nakagawa, Y.; Mizuno, N. *Angew. Chem., Int. Ed.* **2001**, *41*, 3639−3641. (b) Okun, N. M.; Anderson, T. M.; Hill, C. L. *J. Am. Chem. Soc.* **2003**, *125*, 3194−3195. (c) Okun, N. M.; Anderson, T. M.; Hill, C. L. *J. Mol. Catal.* **2003**, *197*, 283−290. (d) Okun, N. M.; Ritorto, M. D.; Anderson, T. M.; Apkarian, R. P.; Hill, C. L. *Chem. Mater.* **2004**, 16, 2551−2558.
(16) Tézé, A.; Hervé, G. In *Inorganic Syntheses*; Ginsberg, A. P., Ed.; John Wiley and Sons: New York, 1990; Vol. 27, pp 85−96.

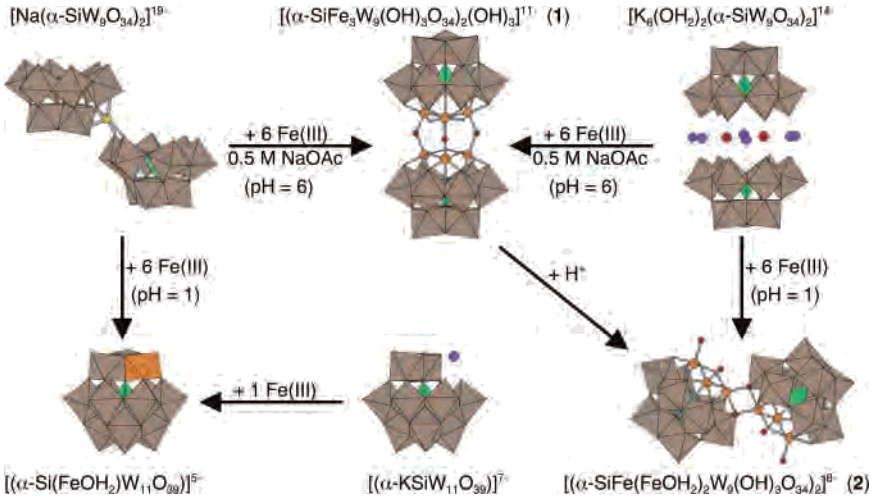


**Figure 2.** Schematic summarizing the reactions of α-$SiW_9O_{34}^{10-}$ with Fe(III). Reaction of either the $Na^+$ salt or the $K^+$ salt of α-$SiW_9O_{34}^{10-}$ with Fe(III) at pH = 6 results in the formation of complex **1**. In contrast, complex **2** is formed by the reaction of Fe(III) and the $K^+$ salt of α-$SiW_9O_{34}^{10-}$ at pH 1. All of the compounds shown here were formulated on the basis of their solid state structures (determined by X-ray crystallography) except [(α-$Si(FeOH_2)W_{11}O_{39}$)]$^{5-}$. The $K^+$ and $Na^+$ counterions not intimately associated with the polyanion moieties were omitted for clarity.

1200−400 $cm^{-1}$): 1001 (w), 955 (m), 904 (s), 940 (s), 776 (s), 709 (m), 629 (w), and 530 (w). Electronic spectral data (400−700 nm, in $H_2O$ (2.5 mM sample, 1 cm cell path length)) [$\lambda$, nm ($\epsilon$, $M^{-1}$ $cm^{-1}$)]: 456 nm (104). Magnetic susceptibility: $\mu_{eff}$ = 9.1 $\mu_B$/mol at 295 K. Anal. Calcd for $K_2Na_6[(Si(FeOH_2)_2FeW_9(OH)_3O_{34})_2]\cdot 8H_2O$ (for a sample dried in vacuo for 12 h): Fe, 6.39; K, 1.49; Na, 2.63; ($OH_2$), 2.7; Si, 1.07; W, 63.1. Found: Fe, 6.44; K, 1.51; Na, 2.60; ($OH_2$), 2.9; Si, 1.04; W, 62.2. [MW = 5245 g/mol].

**X-ray Crystallography.** Single-crystal X-ray crystallographic analyses of **1** and **2** were performed at 100 K on a Brüker D8 SMART APEX CCD sealed tube diffractometer with graphite monochromated Mo Kα (0.71073 Å) radiation according to our previously described methods.[17] Data collection, indexing, and initial cell refinements were carried out using SMART software.[18] Frame integration and final cell refinements were carried out using SAINT software.[19] Final cell parameters were determined from least-squares refinement on 7064 reflections for **1** and 7394 reflections for **2**. Absorption corrections for each data set were applied using SADABS.[20] The structures were determined using direct methods and difference Fourier techniques. A complete list of atoms refined anisotropically is provided in the Supporting Information. No H atoms associated with the water molecules of **1** and **2** were located in the difference Fourier maps. The final R1 scattering factors and anomalous dispersion corrections were taken from *International Tables for X-ray Crystallography*.[21] Structure solution, refinement, and generation of publication materials were performed using SHELXTL V6.12 software. Additional details are provided in Table 1, and thermal ellipsoid plots are given in the Supporting Information (Figures S2 and S3).

**Table 1.** Crystallographic Data and Structure Refinement for **1** and **2**

| | **1** | **2** |
|---|---|---|
| empirical formula | $H_{80.2}Fe_6K_4Na_7O_{112.6}Si_2W_{18}$ | $H_{60.8}Fe_6K_2Na_6O_{101.4}Si_2W_{18}$ |
| fw | 5900.35 | 5600.41 |
| space group | *C*2/*c* | *C*2/*c* |
| unit cell | *a* = 22.454(2) Å | *a* = 36.903(2) Å |
| | *b* = 12.387(2) Å | *b* = 13.9868(9) Å |
| | *c* = 37.421(2) Å | *c* = 21.7839(13) Å |
| | $\beta$ = 100.107(8)° | $\beta$ = 122.709(1)° |
| *V* | 10246.8(15) $Å^3$ | 9460.8(10) $Å^3$ |
| *Z* | 4 | 4 |
| *d* (calcd) | 3.825 g $cm^{-3}$ | 3.932 g $cm^{-3}$ |
| *T* | 100(2) K | 100(2) K |
| $\lambda$ | 0.71073 Å | 0.71073 Å |
| $\mu$ | 2.1278 $cm^{-1}$ | 2.2936 $cm^{-1}$ |
| GOF | 1.200 | 1.022 |
| final $R_1$[a] [$I > 2\sigma(I)$] | 0.0511 | 0.0457 |
| final $wR_2$[b] [$I > 2\sigma(I)$] | 0.1094 | 0.1104 |

[a] $R_1 = \sum||F_o| - |F_c||/|F_o|$. [b] $wR_2 = \{\sum[w(F_o^2 - F_c^2)^2]/\sum[w(F_o^2)^2]\}^{0.5}$.

## Results and Discussion

**Syntheses.** The green, crystalline mixed $K^+/Na^+$ salt of $[(\alpha\text{-}SiFe_3W_9(OH)_3O_{34})_2(OH)_3]^{11-}$ (**1**) is readily prepared in ~70% yield by adding either the $Na^+$ salt or the $K^+$ salt of α-$SiW_9O_{34}^{10-}$ to a solution of exactly 3 equiv of Fe(III) per α-$SiW_9O_{34}^{10-}$ (or 6 equiv of Fe(III) per $[Na(\alpha\text{-}SiW_9O_{34})_2]^{19-}$ or $[K_6(OH_2)_2(\alpha\text{-}SiW_9O_{34})_2]^{14-}$) in 0.5 M sodium acetate. The final pH of this solution prior to isolation of **1** via precipitation with KCl is ~6. Reaction of the $K^+$ salt of α-$SiW_9O_{34}^{10-}$ with 3 equiv of Fe(III) (or 6 equiv of Fe(III) per dimer of $[K_6(OH_2)_2(\alpha\text{-}SiW_9O_{34})_2]^{14-}$) in water (pH = 1) yields $[(\alpha\text{-}Si(FeOH_2)_2FeW_9(OH)_3O_{34})_2]^{8-}$ (**2**). In contrast, the use of the $Na^+$ salt of α-$SiW_9O_{34}^{10-}$ in this reaction gives only $[\alpha\text{-}Si(FeOH_2)W_{11}O_{39}]^{5-}$ due to the rapid decomposition of the POM at pH = 1 (Figure 2).

Previously, the reaction of Fe(III) with the $Na^+$ salt of α-$SiW_9O_{34}^{10-}$ was studied by Pope and co-workers.[7] In their procedure, a slight excess of Fe(III) was used (3.3 Fe(III) to 1 $[SiW_9O_{34}]^{10-}$ versus 3.0 to 1 in this manuscript). The result is that the pH of the solution is slightly lower than 6 since the 0.5 M sodium acetate solution formally buffers (in the presence of the acidic Fe(III) cations) at lower pH ($pK_a$ = 4.76). However, complex **1** is only stable in the range pH 6−7. Acidification of **1** below pH 6 starts the formation of

(17) Anderson, T. M.; Zhang, X.; Hardcastle, K. I.; Hill, C. L. *Inorg. Chem.* **2002**, *41*, 2477−2488.
(18) *SMART*, version 5.624; Brüker AXS, Inc.: Madison, WI, 2002.
(19) *SAINT*, version 6.36A; Brüker AXS, Inc.: Madison, WI, 2002.
(20) Sheldrick, G. *SADABS*, version 2.10; University of Göttingen: Göttingen, Germany, 2003.
(21) *International Tables for X-ray Crystallography*; Kynoch Academic Publishers: Dordrecht, The Netherlands, 1992; Vol. C.

**2**, and the reaction of **1** to **2** is complete upon reaching pH 1. Complex **2** is stable from pH 1−7 so conversion back to **1** is not possible under these conditions. These results are consistent with observations by Pope that small to modest amounts of the dimeric complex were detected by mass spectrometry since a mixture of both complexes forms below pH 6.[7]

Previously, Lunk and co-workers have shown that the addition of 1 M NaOH to a solution of $[(\alpha\text{-Si}(\text{CrOH}_2)_3\text{W}_9(\text{OH})_3\text{O}_{34})]^{4-}$ followed by refluxing results in the formation of the chromium analogue of **1**, $[(\alpha\text{-SiCr}_3\text{W}_9(\text{OH})_3\text{O}_{34})_2(\text{OH})_3]^{11-}$.[22] Interestingly, the addition of 1 M NaOH to complex **2** results in either no change up to pH 7 (as monitored by UV−vis and infrared spectroscopy) or decomposition of the POM at pH > 7. Furthermore, Keggin dimers of $d^0$ metals such as Ti(IV) and Nb(V) (isostructural to **1**) form by acidification of the trisubstituted monomers rather than the addition of base as observed for the dimers with d-electron-containing cations.[23] This is consistent with the fact that the former species (Cr(III) and Fe(III)) have terminal hydroxo (or water) ligands rather than $O^{2-}$.

**Crystallographic Studies.** The structure of complex **1** is shown in Figure 1. The new complex is formed by two A-type $[\alpha\text{-SiFe}_3\text{W}_9(\text{OH})_3\text{O}_{34}]^{4-}$ units linked by three Fe−$\mu$-OH−Fe bonds. Three $\text{Fe}(\text{OH})_3\text{O}_3$ octahedra in each $[\alpha\text{-SiFe}_3\text{W}_9(\text{OH})_3\text{O}_{34}]^{4-}$ unit replace the three corner-sharing $\text{WO}_6$ octahedra missing in $[\text{SiW}_9\text{O}_{34}]^{10-}$. The point group of complex **1** is $\sim D_{3h}$. Originally, crystals of **1** were grown at pH 6. The *R* value of this structure was around 10%. However, when the crystals were regrown at pH ∼6.5, the *R* value improved to ∼5%. Bond valence sum (BVS) calculations for Fe1, Fe2, and Fe3 (see Figure 1 for the numbering scheme) yield average oxidation states of 3.07, 3.06, and 3.04 (± 0.08), respectively.[24] Furthermore, BVS calculations show that hydroxo bridges are also present between adjacent Fe(III) centers in each $[\alpha\text{-SiFe}_3\text{W}_9(\text{OH})_3\text{O}_{34}]^{4-}$ unit (average value for the bridging hydroxo is 1.2 ± 0.1). Complex **1** is the first structurally characterized dimer of triferric Keggin units. However, both *anti* and *syn* isomers are known for diferric Keggin dimers (Figure 3A,B, respectively).[25,26]

The structure of complex **2** is shown in Figure 1. Similar to complex **1**, two $\text{Fe}(\text{OH})_2(\text{OH}_2)\text{O}_3$ octahedra (and one $\text{Fe}(\text{OH})_2\text{O}_3$) in each $[\alpha\text{-Si}(\text{FeOH}_2)_2\text{FeW}_9(\text{OH})_3\text{O}_{34}]^{4-}$ unit replace the three corner-sharing $\text{WO}_6$ octahedra missing in $[\text{SiW}_9\text{O}_{34}]^{10-}$. However, the two $[\alpha\text{-Si}(\text{FeOH}_2)_2\text{FeW}_9(\text{OH})_3\text{O}_{34}]^{4-}$ Keggins are linked by a single edge rather than three Fe−$\mu$-OH−Fe bonds. The single junction between the two $[\alpha\text{-Si}(\text{FeOH}_2)_2\text{FeW}_9(\text{OH})_3\text{O}_{34}]^{4-}$ units contains the $\text{Fe}_2\text{O}_2$ diamondoid structural unit prevalent in several redox metalloenzymes.[27] The terminal coordination site on Fe1 in each trisubstituted Keggin unit shares a bridging oxo ligand with a $[\text{WO}_6]^{2-}$ moiety. Edge-sharing junctions in Keggin dimers are rare as a majority of complexes structurally characterized to date have exclusively corner-sharing junctions. One notable exception is the complex $[(\beta\text{-SiNi}_2\text{W}_{10}\text{O}_{36}(\text{OH})_2(\text{OH}_2))_2]^{12-}$, reported by Kortz.[28] This dimer has two $[\beta\text{-SiNi}_2\text{W}_{10}\text{O}_{36}(\text{OH})_2(\text{OH}_2)]^{6-}$ units linked by their rotated $\text{Ni}(\text{OH})\text{W}_2\text{O}_{12}$ caps (Figure 3C). The point group of complex **2** is $\sim C_i$, and bond valence sum (BVS) calculations for Fe1, Fe2, and Fe3 (see Figure 1 for the numbering scheme) yield average oxidation states of 3.06, 3.05, and 3.07 (±0.08), respectively.[24] Like complex **1**, BVS calculations on **2** also show that hydroxo bridges are present between adjacent Fe(III) centers in each $[\alpha\text{-Si}(\text{FeOH}_2)_2\text{FeW}_9(\text{OH})_3\text{O}_{34}]^{4-}$ moiety (average value for the bridging hydroxo is 1.2 ± 0.1). Select bond lengths (Å) and bond angles (deg) for complexes **1** and **2** are given in Table 2.

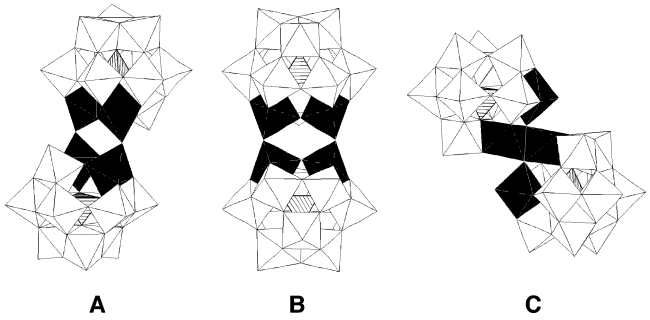


**Figure 3.** Polyhedral representations of (A) *anti*-$[(\text{PW}_{10}\text{O}_{37})_2\text{Fe}_4(\text{OH})_4]^{10-}$, (B) *syn*-$[(\text{SiW}_{10}\text{O}_{37})_2\text{Fe}_4(\text{OH})_4]^{12-}$, and (C) $[(\beta\text{-SiNi}_2\text{W}_{10}\text{O}_{36}(\text{OH})_2(\text{OH}_2))_2]^{12-}$.

**Table 2.** Selected Bond Lengths (Å) and Bond Angles (deg) for **1** and **2**

| | **1** | **2** |
|---|---|---|
| W═$O_{av}$ | 1.724(8) | 1.718(8) |
| Si−$O_{av}$ | 1.641(8) | 1.635(8) |
| Fe···Fe | 3.713 | 3.611 |
| Fe−$OH_2$ | | 2.037 |
| Fe1···Fe2···Fe3 | 61.0 | 59.1 |
| W1···W2···W3 | 59.9 | 60.4 |

**Physical Properties.** The UV−vis spectra of **1** and **2** allow for the clear distinction of the two complexes in solution. The dark green complex **1** displays a $\lambda_{max}$ for the Fe(III)-centered d−d transitions at 436 nm ($\epsilon$ = 146 $M^{-1}$ $cm^{-1}$) (Figure 4). In contrast, the Fe(III)-centered d−d transitions for the yellow-orange complex **2** have a $\lambda_{max}$ at 456 nm ($\epsilon$ = 104 $M^{-1}$ $cm^{-1}$). Both complexes show intense oxygen-to-tungsten-charge-transfer bands in the UV region charac-

(22) Wassermann, K.; Palm, R.; Lunk, H.-J.; Fuchs, J.; Steinfeldt, N.; Stösser, R. *Inorg. Chem.* **1995**, *34*, 5029−5036.
(23) (a) Yamase, T.; Ozeki, T.; Sakamoto, H.; Nishiya, S.; Yamamoto, A. *Bull. Chem. Soc. Jpn.* **1993**, *66*, 103−108. (b) Lin, Y.; Weakley, T. J. R.; Rapko, B.; Finke, R. G. *Inorg. Chem.* **1993**, *32*, 5095−5101. (c) Kim, G.-S.; Zeng, H.; Rhule, J. T.; Weinstock, I. A.; Hill, C. L. *J. Chem. Soc., Chem. Commun.* **1999**, 1651−1652. (d) Nomiya, K.; Takahashi, M.; Ohsawa, K.; Widegren, J. A. *J. Chem. Soc., Dalton Trans.* **2001**, 2872−2878. (e) Kim, G.-S.; Zeng, H.; Neiwert, W. A.; Cowan, J. J.; VanDerveer, D.; Hill, C. L.; Weinstock, I. A. *Inorg. Chem.* **2003**, *42*, 5537−5544.
(24) Brown, I. D.; Altermatt, D. *Acta Crystallogr.* **1985**, *B41*, 244−247.
(25) Li, M.-X.; Jin, S.-L.; Liu, H.-Z.; Xie, G.-Y.; Chen, M.-Q.; Xu, Z.; You, X.-Z. *Polyhedron* **1998**, *17*, 3721−3725.
(26) Tézé, A.; Vaissermann, J. *C. R. Acad. Sci.* **2000**, *3*, 101−105.
(27) Select references on MMO include: (a) Tshuva, E. Y.; Lippard, S. J. *Chem. Rev.* **2004**, *104*, 987−1011. (b) Bassan, A.; Blomberg, M. R. A.; Siegbahn, P. E. M.; Que, Lawrence, Jr. *J. Am. Chem. Soc.* **2002**, *124*, 11056-11063. (c) Costas, M.; Chen, K.; Que, L., Jr. *Coord. Chem. Rev.* **2000**, *200−202*, 517−544. (d) Payne, S. C.; Hagen, K. S. *J. Am. Chem. Soc.* **2000**, *122*, 6399−6410. (e) Lipscomb, J. D.; Que, L., Jr. *J. Biol. Inorg. Chem.* **1998**, *3*, 331−336.
(28) Kortz, U.; Jeannin, Y. P.; Tézé, A.; Hervé, G.; Isber, S. *Inorg. Chem.* **1999**, *38*, 3670−3675.

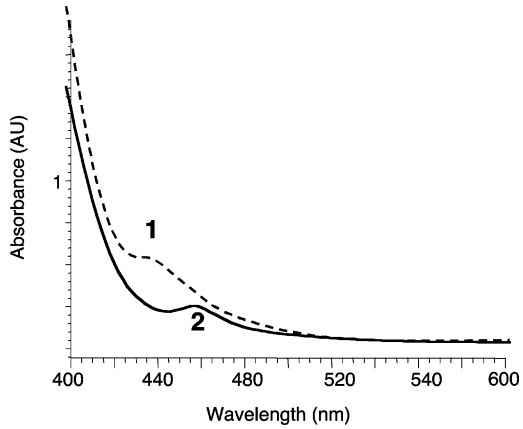


**Figure 4.** Electronic spectra of a 4 mM solution (1 cm cell path length) of complex **1** (- - -) and a 2.5 mM solution (1 cm cell path length) of complex **2** (—).

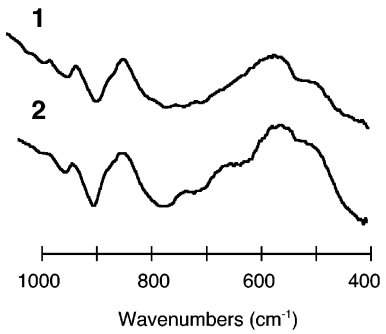


**Figure 5.** Infrared spectra of complex **1** (top) and complex **2** (bottom). Both samples display the bands typical of Keggin silicotungstates between 1000 and 800 $cm^{-1}$, but subtle distinctions are present between the two complexes from 800 to 600 $cm^{-1}$.

teristic of all $d^0$ POMs. The infrared spectra of both **1** and **2** show the bands typical of Keggin silicotungstates at 1000, 950, 900, and 800 $cm^{-1}$ (Figure 5).[29] However, there are subtle differences observed in the bands between 800 and 600 $cm^{-1}$ which distinguish each of the two complexes. The ambient-temperature magnetic moments of **1** (8.1 $\mu_B$/mol) and **2** (9.1 $\mu_B$/mol) imply some degree of antiferromagnetic coupling. The effective spin-only moment for a fully ferromagnetically coupled $S = 15$ system is 30.9 $\mu_B$. The paramagnetic ground electronic state of the six Fe(III) cations in **1** and **2** precludes the acquisition of $^{29}Si$ and $^{183}W$ NMR.

**Stability Studies.** Differential scanning calorimetry (DSC) data on solid crystalline samples of **1** and **2** show a number of endotherms below 300 °C (Figure 6). Thermogravimetric analyses (TGA) of the same samples establish that these peaks correspond to the loss of lattice water molecules (approximately 8.4% and 2.9% by mass for complexes **1** and **2**, respectively). Finally, there is an exothermic process observed in complex **1** (from 575 to 600 °C) that is attributable to the decomposition of the POM. The thermal data are corroborated by the observation of significant changes in the infrared spectra of **1** upon heating of the

(29) (a) Rocchiccioli-Deltcheff, C.; Thouvenot, R. *J. Chem. Res., Synop.* **1977**, *2*, 46−47. (b) Rocchiccioli-Deltcheff, C.; Fournier, M.; Franck, R.; Thouvenot, R. *Inorg. Chem.* **1983**, *22*, 207−216. (c) Thouvenot, R.; Fournier, M.; Franck, R.; Rocchiccioli-Deltcheff, C. *Inorg. Chem.* **1984**, *23*, 598−605.

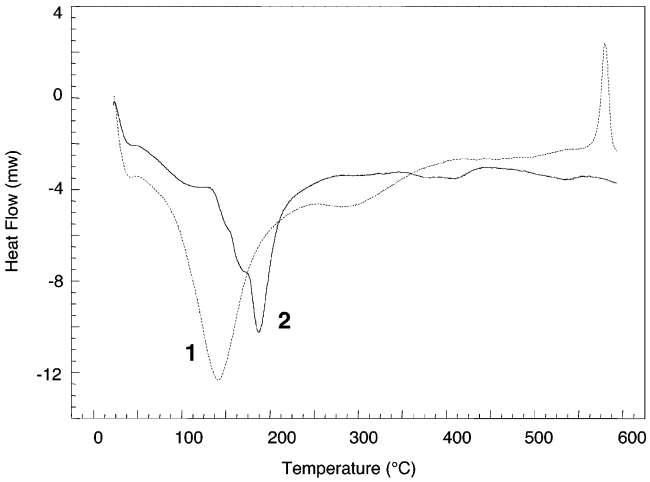


**Figure 6.** Differential scanning calorimetry (DSC) data for complexes **1** (- - -) and **2** (—). Crystalline samples (10 mg) were previously dried in vacuo for 12 h and then heated from 25 to 600 °C at a rate of 20 °C/min.

sample to 600 °C. Interestingly, no decomposition of complex **2** is observed by DSC or FT-IR up to temperatures of 600 °C. Presumably, this is due in part to the lower overall negative charge of complex **2** (8− versus 11− for complexes **2** and **1**, respectively). However, examination of the bond lengths and angles summarized in Table 2 reveals there are modest perturbations in the coordination environments of W(VI) and Fe(III) in $[\alpha\text{-}SiFe_3W_9(OH)_3O_{34}]^{4-}$ due to the formation of the two different dimeric structures.

The stability of complexes **1** and **2** was also evaluated in solution. The natural pH of a 5 mM solution of **1** is 7. Heating a 10 mM solution of **1** to 90 °C results in the solution changing from dark green to bright orange. In addition, the pH of the solution increases to 8.5. Addition of 1 M HCl to this solution quickly regenerates the dark green color of the starting complex. The natural pH of a 5 mM solution of complex **2** is 3. Heating a 10 mM solution of **2** to 90 °C (with the pH adjusted to 7 by the addition of NaOH) does not give a color change. However, the bright orange color does appear if the pH is raised to 8.5. Attempts to obtain crystals of this orange complex have not yet been successful.

One interesting aspect of the chemistry of complex **2** is whether it retains the dimeric structure in solution. In this compound, one of the three Fe(III) centers in each Keggin subunit is bound to an oxo ligand from the other Keggin unit. There are three lines of evidence to suggest that complex **2** most likely does not exist as a dimer in solution but probably is the monomeric species $[SiFe_3(OH)_3W_9O_{34}]^{4-}$. First, the structure of **2** has two $Fe(OH)_2(OH_2)O_3$ octahedra and one $Fe(OH)_2O_3$ which should lead to two different $\lambda_{max}$ in the electronic spectra. However, there is only one $\lambda_{max}$ suggesting that the three Fe(III) centers are equivalent (Figure 4). Second, although the paramagnetism of the six Fe(III) centers precluded the acquisition of $^{183}W$ NMR, diffraction quality crystals of complex **2** (grown at pH ∼1.0) were regrown at pH ∼3.5. The structure of the triferric POM grown at the higher pH is clearly a monomer. These crystals have both crystallographically imposed symmetry disorder and positional disorder that is endemic to substituted Keggin POMs. Both of these phenomena have plagued many

attempted structure determinations of α Keggin POMs (α-$XM_{12}O_{40}$, X = heteroatom and M = combination of 75% W(VI) and 25% Fe(III), for example).[30] Finally, there is some literature precedence for this type of binding and equilibrium (essentially a monomer in solution and dimer in the solid state). For example, Francesconi and co-workers have shown by $^{183}W$ NMR spectroscopy and luminescence lifetime measurements that $[(Eu(OH_2)_3(\alpha_2\text{-}P_2W_{17}O_{61}))_2]^{14-}$, in which two identical POM moieties are bound through two Eu−$\mu$-O═W linkages, dissociates in solution to form the monomeric species $[(Eu(OH_2)_4(\alpha_2\text{-}P_2W_{17}O_{61}))]^{7-}$.[31]

Finally, we have assessed the stability of **1** and **2** in organic solvents (acetone, acetonitrile, and methylene chloride). Organic solvent soluble forms of these POMs are readily obtained by adding a phase transfer reagent (such as Aliquat 336) to an aqueous solution of **1** or **2**, followed by extraction into methylene chloride. Regardless of the starting material (**1** or **2**), the UV−vis and infrared spectroscopic data suggest that the same complex is obtained. This product is a match for the pure tetra-*n*-butylammonium salt of $[\alpha\text{-}SiFe_3W_9(OH)_3O_{34}]^{4-}$ reported by Mizuno.[32] The instability of Fe(III)−POM dimers in organic solvents was previously studied by Tourné.[33] They have shown that the equilibrium between the monosubstituted $[\alpha\text{-}SiFeW_{11}O_{39}]^{5-}$ complex and its dimeric form, $[(\alpha\text{-}SiFeW_{11}O_{39})_2(O)]^{12-}$ (or $[(\alpha\text{-}SiFeW_{11}O_{39})_2(OH)]^{11-}$), strongly favors the formation of the monomer as the ratio of water to methanol is decreased.[34]

**Acknowledgment.** We would like to thank the National Science Foundation (Grant CHE-0236686) and the Army Research Office (Grant DAMD17-99-C-9012) for funding.

**Supporting Information Available:** Structure determination parameters, crystal and structure refinement data, and atomic coordinates and isotropic displacement parameters for **1** and **2** (in CIF form); thermal ellipsoid plots for **1** and **2**, and combination polyhedral/ball-and-stick illustrations of $[Na_{10}(\beta\text{-}SiW_9O_{34})_2]^{10-}$, $[Na_8(\beta\text{-}PW_9O_{34})_2]^{10-}$, and $[K_3(\alpha\text{-}Si_2W_{18}O_{66})]^{13-}$ (as a pdf). This material is available free of charge via the Internet at http://pubs.acs.org.

IC049517S

(30) See, for example: Evans, H. T., Jr.; Pope, M. T. *Inorg. Chem.* **1984**, *23*, 501−504.
(31) Luo, Q.; Howell, R. C.; Bartis, J.; Dankova, M.; Horrocks, W. DeW., Jr.; Rheingold, A. L.; Francesconi, L. C. *Inorg. Chem.* **2002**, *41*, 6112−6117.
(32) Mizuno, N.; Nozaki, C.; Kiyoto, I.; Misono, M. *J. Am. Chem. Soc.* **1998**, *120*, 9267−9272.
(33) Zonnevijlle, F.; Tourné, C. M.; Tourné, G. F. *Inorg. Chem.* **1982**, *21*, 2751−2757.
(34) Recently, Mialane et al. studied the oligomerization of $[SiCu_3(OH)_3W_9O_{34}]^{7-}$ (in the presence of $N_3^-$) to form $\{[(SiW_9O_{34})(SiW_9O_{33}(OH))(Cu(OH))_6Cu]_2X\}^{23-}$ (X = $Cl^-$ or $Br^-$). See: Mialane, P.; Dolbecq, A.; Marrot, J.; Rivière, E.; Sécheresse, F. *Angew. Chem., Int. Ed.* **2003**, *42*, 3523−3526.